Tissue Engineering

DOI: 10.1089/ten.TEA.2019.0058

Heparan sulfate mimetics accelerate post-injury skeletal muscle regeneration

Jessica Bouvière[1,5], MSc; Aurélie Trignol[1,2,5], MD, PhD; Dieu-Huong Hoang[1], MSc; Peggy del Carmine[1], MSc; Marie-Emmanuelle Goriot[2], BSc; Sabrina Ben Larbi[1], BSc; Denis Barritault[3,4], PhD; Sébastien Banzet[2], MD, PhD; Bénédicte Chazaud[1,5], PhD.

1- Univ Lyon, Université Claude Bernard Lyon 1, CNRS UMR-5310, INSERM U-1217, Institut NeuroMyoGène, 8 Avenue Rockefeller, 69008, Lyon, France

2- Institut de Recherche Biomédicale des Armées, Département Soutien Médico-Chirurgical des Forces, UMR-MD-1197, 1 rue du lieutenant Raoul Batany, 92140, Clamart, France

3- OTR3, 4 rue Française, 75001, Paris, Fance

4- Laboratoire CRRET, Université Paris-Est Creteil, 94000 Créteil, France

5- Equally contributed to the work

6- Corresponding author

Jessica Bouvière	jessica.bouviere@univ-lyon1.fr	+33 426 688 249
Aurélie Trignol	aurelie.trignol@inserm.fr	+33 426 688 249
Dieu-Huong Hoang	dieu-huong.hoang@univ-lyon1.fr	+33 426 688 249
Peggy del Carmine	peggy.del-carmine@univ-lyon1.fr	+33 426 688 249
Marie-Emmanuelle Goriot	marie-emmanuelle.goriot@inserm.fr	+33 141 467 260
Sabrina Ben Larbi	sabrina.ben-larbi@univ-lyon1.fr	+33 426 688 249
Denis Barritault	denis.barritault@otr3.com	+33 664 100 550
Sébastien Banzet	sebastien.banzet@inserm.fr	+33 141 467 260
Bénédicte Chazaud	benedicte.chazaud@inserm.fr	+33 426 688 249

Tissue Engineering
Heparan sulfate mimetic accelerate post-injury skeletal muscle regeneration (DOI: 10.1089/ten.TEA.2019.0058)
This paper has been peer-reviewed and accepted for publication, but has yet to undergo copyediting and proof correction. The final published version may differ from this proof.

Abstract 100-200 words

Although skeletal muscle is capable of complete recovery after an injury, specific situations requires support or acceleration of this process, such as in elderly and athlete, respectively. Skeletal muscle regeneration is due to muscle stem cells that undergo adult myogenesis, a process sustained by muscle stem cell environment. Although recognized as important, extracellular matrix (ECM) has been overlooked in this process. Matrix-based therapy aims at improving ECM remodeling to support tissue repair. In this context, we investigated the properties of a single injection of the clinical grade glycosaminoglycan mimetics RGTA® (ReGeneraTing Agents) on skeletal muscle regeneration in a context compatible with a clinical application, *i.e.*, three days after the injury. Our results show that RGTA®-treated muscles showed an increase of the number of myonuclei in regenerating myofibers and an increase of the capillarization of the new myofibers. In vitro experiments showed that RGTA® directly acts on muscle stem cells by stimulating their fusion into myotubes and on endothelial cells by stimulating the formation and maturation of vessels in a 3D culture set up. These results indicate that a single administration of RGTA® in regenerating muscle stimulated both myogenesis and angiogenesis, thus accelerating skeletal muscle regeneration.

Impact statement

Although highly powerful in normal condition, post-injury skeletal muscle regeneration is less efficient in some situations, such as obese, elderly or resting people. In other context, such as high-performance sport, skeletal muscle regeneration must be shortened but in a way ensuring a full functional recovery. In this context, our results show that a single injection of the clinical grade glycosaminoglycan mimetics RGTA® (ReGeneraTing Agents) in a context compatible with a clinical application, i.e. three days after the injury is beneficial for skeletal muscle regeneration, through the stimulation of both myogenesis and angiogenesis.

Tissue Engineering
Heparan sulfate mimetic accelerate post-injury skeletal muscle regeneration (DOI: 10.1089/ten.TEA.2019.0058)
This paper has been peer-reviewed and accepted for publication, but has yet to undergo copyediting and proof correction. The final published version may differ from this proof.

Introduction

Adult skeletal muscle is highly adaptable to the physiological demand. Moreover, skeletal muscle is capable of complete recovery after an injury, thanks to the activation of muscle stem cells (MuSCs) that activate, expand, differentiate and finally fuse to form new functional myofibers (1). While historical investigations have focused on MuSCs, which are indispensable for muscle regeneration, more recent studies have evidenced that their environment is equally important for the efficacy of the regeneration process (2, 3). MuSC environment encompasses several cell types as well as the extracellular matrix (ECM) which has been overlooked in the regeneration process. Indeed, much attention has focused on the pathological development of excessive ECM, which is fibrosis (4), but the physiological roles of ECM remodeling remains poorly understood. The mechanisms by which ECM components support skeletal muscle regeneration are still largely unknown, due to technical limitations for the study of the large and insoluble ECM proteins and glycoproteins. Nevertheless, attempts have been made to manipulate skeletal muscle ECM in order to improve muscle repair, notably through the use of ECM scaffolds to restore volumetric muscle loss (5).

Matrix-based therapy aims at improving ECM remodeling to support tissue repair. In this context, components such as RGTA® for ReGeneraTing Agents include polymeric molecules that bind growth factors and cytokines and modulate their activity. Glycosaminoglycan mimetics mimic their capacities to sequester and present soluble factors to their receptors (6, 7). RGTA® are resistant to enzymatic degradation, and replace heparan sulfates (HS) at heparan-binding sites in the matrix, allowing the ECM scaffold and growth factors to reposition in the cellular microenvironment (7). Among the latest developed RGTA® are dextran polymers, harboring controlled sulfated or controlled sulfated carboxymethyl and acetylated groups and acting as an HS mimetic (7, 8), that has proven to improve repair of various tissues including skin (9), bone (10), tendon (11), or periodontal tissue (12), with no toxicity (13).

First developed RGTA® were tested in mechanical models of skeletal muscle injury, in healthy rats, where they were injected at the time of the damage. Results have shown an acceleration of the regeneration process assessed by the kinetics of myosin heavy chain

Tissue Engineering
Heparan sulfate mimetic accelerate post-injury skeletal muscle regeneration (DOI: 10.1089/ten.TEA.2019.0058)

expression (14). Injection of RGTA® was also tested in the model of hindlimb critical ischemia that induces muscle injury, where it was also injected at the time of the damage. Results showed a protective effect of RGTA® on myofibers, and an improvement of the muscle repair process, mainly due to an increase of surviving myofibers (15). A clinical grade RGTA® was more recently used in the same context of hindlimb ischemia (16). It was shown that RGTA® increases the number of myonuclei, indicative of beneficial effect on myogenesis, as well as an increase of vessel density, indicative of a beneficial effect on angiogenesis (16). Here again, the administration was concomitant to the injury, preventing to discriminate the effects of RGTA® on cell survival *versus* on tissue repair. Moreover, administration of a therapeutic agent at the time of injury is not translatable to the clinical practice.

To dissect RGTA® effects on skeletal muscle regeneration, we used a defined RGTA® (namely OTR4133 with carboxymethyl sulfate and acetate groups) in a model of toxic injury that targets the whole muscle (on the contrary of mechanical injuries that differentially affects the various parts of the muscle) and which is highly reproducible and well-established in term of kinetics of the biological processes involved (*i.e.*, myogenesis, angiogenesis, inflammation, ECM remodeling). The first phase is the inflammatory phase during which inflammatory cells invade the damaged muscle, clean the tissue debris, and stimulate MuSC expansion (1-3). At the time of the resolution of inflammation (day 2-3), the recovery phase begins, MuSCs exit the cell cycle, proliferate (days 3-4 post-injury) and commit into terminal myogenic differentiation and fuse to form new myofibers (days 6-14) (17). During the recovery phase, the formation of new vessels is observed, since angiogenesis is coupled with myogenesis (18). In the present study, we identified the effects of a single injection of RGTA® at the time of recovery during skeletal muscle regeneration and evaluated the outcomes on regeneration efficiency. Data showed that during the recovery phase, RGTA® administration stimulated MuSC fusion and angiogenesis, accelerating muscle regeneration.

Tissue Engineering
Heparan sulfate mimetic accelerate post-injury skeletal muscle regeneration (DOI: 10.1089/ten.TEA.2019.0058)
This paper has been peer-reviewed and accepted for publication, but has yet to undergo copyediting and proof correction. The final published version may differ from this proof.

MATERIAL AND METHODS

Muscle injury. Adult 9-week-old C57BL/6J male mice were used according to the French legislation. Injury was induced by injecting 50 µl of cardiotoxin (Latoxan, 12 µM) in each Tibialis Anterior muscle as previously described (17). RGTA® (GAG mimetic ([OTR-4133], a close molecule to OTR4131 (11), provided by OTR3 Company, Paris, France), was injected into regenerating muscle 3 days after cardiotoxin injury at 1 µg/10 µl/muscle (control muscle was injected with 10 µl of PBS /muscle). Mice were euthanized 8 and 28 days after injury and muscles were harvested, frozen in liquid nitrogen-precooled isopentane and stored at -80°C. Ten micrometer-thick cryosections were prepared for histological analysis.

Histological staining. Muscle sections were stained with Hematoxylin-Eosin to evaluate the overall regeneration process. Sudan black staining was made to stain lipids: sections were dehydrated in ethanol 70% for 10 sec, stained in Sudan Black solution (Sigma-Aldrich) for 2h, counterstained with Hemalun (Sigma-Aldrich) for 1 min and mounted with Fluoromount-G Mounting Medium (Interchim). The entire muscle section was scanned with an Axio Scan. Z1 microscope (Zeiss) at 20X objective connected to a 3 CCD HV-F 2025 color camera (Hitachi). Stained area was quantified using Image J software and was represented as a percentage of the entire muscle section area.

Histological immunolabeling. Muscle cryosections were treated with primary antibodies as in (18) for the detection of laminin (#L9393, Sigma-Aldrich) and of CD31 (Abcam, ab28364) revealed with Cy3- or FITC-conjugated antibodies (Jackson Immunoresearch Inc). Nuclei were labeled with Hoechst (Sigma-Aldrich). For laminin immunolabeling, the entire cryosections were automatically scanned at X10 objective using an Axio Observer.Z1 (Zeiss) connected to a CoolSNAP HQ2 CCD Camera (photometrics). The image of the whole cryosection was automatically reconstituted in MetaMorph Software. Cross Sectional Area (CSA) was measured using a macro developed under ImageJ software (19). For CD31 evaluation, about 10-12 pictures were recorded at 20x objective. The number of vessels (CD31 positive structures exhibiting a nucleus) and the number of myofibers were counted.

Muscle stem cell culture. MuSCs were extracted from mouse muscle hindlimbs from 3 to 5 weeks of age as described previously (17). Cells were cultured on 2-well permanox

Tissue Engineering
Heparan sulfate mimetic accelerate post-injury skeletal muscle regeneration (DOI: 10.1089/ten.TEA.2019.0058)
This paper has been peer-reviewed and accepted for publication, but has yet to undergo copyediting and proof correction. The final published version may differ from this proof.

chambers (Nunc Lab-Tek) coated with Matrigel Matrix Growth Factor Reduced (Corning, 356231) (1/10). For proliferation assay, MuSCs were seeded at 10000 cell/cm^2 in proliferation medium [DMEM/F12 (Gibco), 20% Fetal Bovine Serum (Gibco) and 2% Ultroser™ G (Pall Inc)] for 6 h, washed 3 times with PBS and were incubated in proliferation medium containing or not RGTA® (10 µg/ml) for 1 day at 37°C. Immunolabeling for Ki67 (Abcam, ab15580) was performed as described in (17). For fusion assay, MuSCs were seeded at 30000 cell/cm^2 in proliferating medium for 6 h then they were switched to differentiation medium [DMEM/F12, 2% horse serum (Gibco)] containing or not RGTA® (10 µg/ml) for 3 days at 37°C. Phalloidin staining (Sigma-Aldrich, P5282) was used to label actin and Hoechst to stain nuclei. Pictures were recorded using a Zeiss Observer Z1 microscope connected to a Coolsnap HQ (Photometrics) camera at 20x magnification. About 6-8 randomly chosen fields were counted. The number of ki67positive cells was expressed as a percentage of total nuclei. The number of nuclei per cell was counted, defining several classes of myotubes. Fusion index was calculated as the number of nuclei within myotubes upon the total number of nuclei.

3D angiogenesis culture assay. 3D culture was carried out as previously described (18). Briefly, HUVECs were infected with lenti-GFP, were seeded on cytodex beads and embedded into a fibrinogen solution. The cells/fibrinogen solution was allowed to clot and form a gel in 8-well glass Lab-Tek. When set, EndoGro medium containing or not RGTA® (10 µg/ml) was added on top of the gel and was changed every 2 days. After 6 days, cultures were captured using a Zeiss Observer Z1 microscope connected to a Coolsnap HQ (Photometrics) camera at 10x objective. Analysis was done with ImageJ software as described in (18).

Statistical analysis. Results are expressed as means ± SEM. Statistical analyses t-tests and ANOVA as described in the figure legends. The number of experiments is indicated in the figure legends.

Tissue Engineering
Heparan sulfate mimetic accelerate post-injury skeletal muscle regeneration (DOI: 10.1089/ten.TEA.2019.0058)
This paper has been peer-reviewed and accepted for publication, but has yet to undergo copyediting and proof correction. The final published version may differ from this proof.

Results and Discussion

RGTA® was *in situ* administrated 3 days post-injury. In this way, the effects of RGTA® were analyzed on the recovery phase of muscle regeneration, that takes place after the inflammatory phase is resolved (20). Days 8 and 28 post injury were chosen to evaluate the direct impact and the long-lasting effects of RGTA® on muscle regeneration, respectively. RGTA® show a dose-dependent effect on tissue repair with a bell-shaped curve (7). Pharmacokinetic studies showed a durable accumulation (8 days) of RGTA® at sites of injury/regeneration when administrated once at the time of the injury, either locally or systemically (21), suggesting that a single injection could be optimal. The dose chosen was adapted from previous studies and results from OTR3 (16).

RGTA® is beneficial to skeletal muscle regeneration by increasing muscle cell fusion and angiogenesis

Cardiotoxin-injected Tibialis Anterior muscles presented a homogenous regeneration pattern indicating that the puncture made at day 3 post-injury (of either saline or RGTA®) did not induce a supplementary locally lasting injury (Figure 1A). At day 8 after injury, there was no difference in weight between the RGTA®-treated and control muscles (Figure 2A). Laminin immunostaining, to label the basal membrane surrounding each myofiber, was made to analyze the number and size of myofibers (Figure 1B). The total number of myofibers was not changed (Figure 2A), neither the size of the myofibers (Figure 2C,D). However, our analysis showed that RGTA® treatment induced an important increase of the number of myonuclei per myofiber (+145%) (Figure 2E) that leaded to the increased number of myofibers presenting 4 or more nuclei on the muscle sections (Figure 2F). This result suggests that RGTA® treatment increased myogenic cell fusion at the time of the formation of new myofibers during muscle regeneration. Sudan Black staining indicated that the area covered by lipids decreased by 60% in RGTA®-treated muscles (Figure 1C, Figure 2G). Lipid accumulation in regenerating muscle is a hallmark of defective regeneration, adipocytes deriving from Fibro-Adipogenic Precursors (FAPs) (22). However, the level of lipid staining was very low even in the control muscles (0.3% of the total muscle area) suggesting no major change in FAP homeostasis. Finally, immunostaining for CD31 (expressed by endothelial cells) was performed to analyze the capillarization of

Tissue Engineering
Heparan sulfate mimetic accelerate post-injury skeletal muscle regeneration (DOI: 10.1089/ten.TEA.2019.0058)

myofibers. The number of capillaries/myofiber was increased by 134% in RGTA®-treated muscles as compared with the control muscles (Figure 1D, Figure 2H), indicating that RGTA® increased angiogenesis during muscle regeneration.

Similar analyses were performed at day 28 after the injury to evaluate the long-lasting effects of RGTA®-treatment (Figure 3). Muscle weight (Figure 4A), myofiber number (Figure 4B) and size of the myofibers (Figure 4C,D) were not changed by RGTA® treatment. The mean number of nuclei in myofibers was normalized between the two conditions (Figure 4E) while the distribution of the myofibers according to their number of myonuclei was still statistically different, indicating that myofibers with high numbers of nuclei were more numerous in RGTA®-treated muscles than in control muscles (Figure 4F). Adiposis staining was very low at day 28 post-injury with no difference between control and RGTA®-treated groups (Figures 3C, 4G). On the contrary, capillarization of the myofibers was still 123% higher in RGTA®-treated muscles than in control muscles (Figures 3D, 4H).

Altogether, these results indicate that RGTA® administration at the time of the resolution of inflammation supported the recovery processes and accelerated muscle regeneration. A previous study reported an increased size of generating myofibers upon RGTA® treatment, the mimetic was administrated at the time of the injury (which was ischemia/denervation) and the treatment was associated with a decrease of cell damage (15). In a similar critical hindlimb ischemia, where the first damage is vascular, RGTA® administration at the time of injury increased the density of myonuclei and that of vessels 8 days after ischemia (16). Our *in vivo* results indicate a long-lasting effect of RGTA® on muscle cell fusion and on angiogenesis during muscle regeneration.

RGTA® directly acts on muscle stem cells and endothelial cells to stimulate myogenesis and angiogenesis *in vitro*

Upon activation after muscle injury (*i.e.*, plating in culture), MuSCs first proliferate to expand, then exit the cell cycle to commit into terminal differentiation to fuse together to form multinucleated myotubes, which prefigure the myofibers *in vitro*. MuSC proliferation and differentiation/fusion are regulated by opposite molecular mechanisms (1). To confirm the above *in vivo* observations at the cell level *in vitro*, culture experiments were performed in the presence of RGTA®. *In vitro* and *in vivo* comparisons are difficult to make

Tissue Engineering
Heparan sulfate mimetic accelerate post-injury skeletal muscle regeneration (DOI: 10.1089/ten.TEA.2019.0058)
This paper has been peer-reviewed and accepted for publication, but has yet to undergo copyediting and proof correction. The final published version may differ from this proof.

since the accessibility of the cells to the compound *in vivo* is difficult to assess. We therefore tested a range of RGTA® concentrations to investigate its effect on MuSC fusion, since the major outcome observed *in vivo* was an increase of the number of myonuclei per myofiber. Myotubes were identified as structures containing several nuclei after staining for the ubiquitous cytoskeletal component actin (Figure 5A,B). Our results show that a concentration of 10 μg/ml of RGTA® produced the most consistent effect on several primary cells (data not shown) and was chosen. In accordance with the increased number of myonuclei in regenerating myofibers in RGTA®-treated muscles *in vivo*, RGTA® stimulated MuSC fusion (+145%), dramatically increasing the appearance of myotubes exhibiting high number of nuclei (Figure 5A,B). Consistently, RGTA® induced a decrease of the proliferation of MuSCs (-19%) (Figure 5C,D) that was evaluated after immunostaining for ki67 that labels cycling cells. These results show that RGTA® directly promotes MuSC fusion, in accordance with the *in vivo* results. Previous studies, using either cell lines or rat primary cells, showed that the effects of RGTA® are dose-dependent, and for the efficient concentrations, promotes both cell growth and fusion that were analyzed in the same experiment (23-25). RGTA® proliferative effect was mainly driven through its potentiating effect of FGFb on MuSCs (24). Similarly, RGTA® was shown to increase angiogenesis through the potentiation of VEGF properties (26). We took advantage of a 3D angiogenesis model in which GFP-labelled human endothelial cells are allowed to form new vessels that further lumenize, indicative of their differentiation and the maturation of the newly formed capillaries (18). Using this device, we showed that RGTA® increased (+168%) the length of capillaries that formed (Figure 4E,F). Moreover, RGTA® triggered the maturation of the sprouting vessels, as assessed by a huge increase of their lumenization (+248%) (Figure 5G). It is to note that in the RGTA® condition, more nuclei are visible within the gel (Figure 5F), indicative of a stimulating effect of RGTA® on endothelial cell proliferation, which was previously reported (26, 27). These results show the direct proangiogenic properties of RGTA® on endothelial cells, in accordance of the increased capillarization observed in the regenerating muscle *in vivo* upon RGTA® treatment.

In conclusion, our study shows that the clinical-grade RGTA® is effective at accelerating muscle regeneration when locally administered at the onset of the regenerating phase, a

clinically compatible time-point. We showed *in vitro* that the main properties of RGTA® are a stimulating effect on MuSC fusion that is required for the formation of new myofibers and on the formation and maturation of new blood vessels. These direct and specific effects of RGTA® on MuSCs and endothelial cells accelerate myogenesis and angiogenesis during muscle regeneration. As a natural HS, RGTA® hold a strong binding capacity for soluble factors providing their stability and their protection against enzymatic degradation (8). Growth factors known to interact with HS include molecules such as FGF, VEGF or TGFβ, which have been involved in both myogenesis and angiogenesis (1). Thus RGTA® compounds may be of interest for accelerating muscle regeneration or healing in specific conditions, for example in athletes, for which this process needs to be shorten.

Acknowledgements

This work was supported by ANR-15-ASTR-0013-01 Myo-MECa, supported by Agence National de la Recherche and Direction Générale des Armées.

Author Disclosure Statement

No competing financial interests exist.”

Reprint author

Institut NeuroMyoGène

UMR CNRS 5310 – INSERM U1217

Universite Claude Bernard Lyon 1

8 Avenue Rockefeller

F-69008 Lyon

Tel: (33) 4 26 68 82 49

benedicte.chazaud@inserm.fr

Tissue Engineering
Heparan sulfate mimetic accelerate post-injury skeletal muscle regeneration (DOI: 10.1089/ten.TEA.2019.0058)
This paper has been peer-reviewed and accepted for publication, but has yet to undergo copyediting and proof correction. The final published version may differ from this proof.

References

1. Yin, H., Price, F., and Rudnicki, M.A. Satellite cells and the muscle stem cell niche. Physiol Rev. 93, 23-67, 2013.

2. Dumont, N.A., Wang, Y.X., and Rudnicki, M.A. Intrinsic and extrinsic mechanisms regulating satellite cell function. Development. 142, 1572-81, 2015.

3. Wosczyna, M.N., and Rando, T.A. A Muscle Stem Cell Support Group: Coordinated Cellular Responses in Muscle Regeneration. Dev Cell. 46, 135-143, 2018.

4. Chapman, M.A., Meza, R., and Lieber, R.L. Skeletal muscle fibroblasts in health and disease. Differentiation. 92, 108-115, 2016.

5. Badylak, S.F., Dziki, J.L., Sicari, B.M., Ambrosio, F., and Boninger, M.L. Mechanisms by which acellular biologic scaffolds promote functional skeletal muscle restoration. Biomaterials. 103, 128-136, 2016.

6. Barbier-Chassefiere, V., Garcia-Filipe, S., Yue, X.L., Kerros, M.E., Petit, E., Kern, P., et al. Matrix therapy in regenerative medicine, a new approach to chronic wound healing. J Biomed Mater Res A. 90, 641-7, 2009.

7. Barritault, D., Desgranges, P., Meddahi-Pelle, A., Denoix, J.M., and Saffar, J.L. RGTA((R))-based matrix therapy - A new branch of regenerative medicine in locomotion. Joint Bone Spine. 84, 283-292, 2017.

8. Rouet, V., Meddahi-Pelle, A., Miao, H.Q., Vlodavsky, I., Caruelle, J.P., and Barritault, D. Heparin-like synthetic polymers, named RGTAs, mimic biological effects of heparin in vitro. J Biomed Mater Res A. 78, 792-7, 2006.

9. Garcia-Filipe, S., Barbier-Chassefiere, V., Alexakis, C., Huet, E., Ledoux, D., Kerros, M.E., et al. RGTA OTR4120, a heparan sulfate mimetic, is a possible long-term active agent to heal burned skin. J Biomed Mater Res A. 80, 75-84, 2007.

10. Frescaline, G., Bouderlique, T., Mansoor, L., Carpentier, G., Baroukh, B., Sineriz, F., et al. Glycosaminoglycan mimetic associated to human mesenchymal stem cell-based scaffolds inhibit ectopic bone formation, but induce angiogenesis in vivo. Tissue Eng Part A. 19, 1641-53, 2013.

11. Jacquet-Guibon, S., Dupays, A.G., Coudry, V., Crevier-Denoix, N., Leroy, S., Sineriz, F., et al. Randomized controlled trial demonstrates the benefit of RGTA(R) based matrix therapy to treat tendinopathies in racing horses. PLoS One. 13, e0191796, 2018.

12. Lallam-Laroye, C., Baroukh, B., Doucet, P., Barritault, D., Saffar, J.L., and Colombier, M.L. ReGeneraTing agents matrix therapy regenerates a functional root attachment in hamsters with periodontitis. Tissue Eng Part A. 17, 2359-67, 2011.

13. Charef, S., Tulliez, M., Esmilaire, L., Courty, J., and Papy-Garcia, D. Toxicological evaluation of RGTA OTR4120, a heparan sulfate mimetic. Food Chem Toxicol. 48, 1965-8, 2010.

14. Aamiri, A., Butler-Browne, G.S., Martelly, I., Barritault, D., and Gautron, J. Influence of a dextran derivative on myosin heavy chain expression during rat skeletal muscle regeneration. Neurosci Lett. 201, 243-6, 1995.

15. Desgranges, P., Barbaud, C., Caruelle, J.P., Barritault, D., and Gautron, J. A substituted dextran enhances muscle fiber survival and regeneration in ischemic and denervated rat EDL muscle. Faseb J. 13, 761-6, 1999.

16. Chevalier, F., Arnaud, D., Henault, E., Guillevic, O., Sineriz, F., Ponsen, A.C., et al. A fine structural modification of glycosaminoglycans is correlated with the progression of muscle regeneration after ischaemia: towards a matrix-based therapy? Eur Cell Mater. 30, 51-68, 2015.

17. Theret, M., Gsaier, L., Schaffer, B., Juban, G., Ben Larbi, S., Weiss-Gayet, M., et al. AMPKalpha1-LDH pathway regulates muscle stem cell self-renewal by controlling metabolic homeostasis. Embo J. 36, 1946-1962, 2017.

Tissue Engineering
Heparan sulfate mimetic accelerate post-injury skeletal muscle regeneration (DOI: 10.1089/ten.TEA.2019.0058)
This paper has been peer-reviewed and accepted for publication, but has yet to undergo copyediting and proof correction. The final published version may differ from this proof.

18. Latroche, C., Weiss-Gayet, M., Muller, L., Gitiaux, C., Leblanc, P., Liot, S., et al. Coupling between Myogenesis and Angiogenesis during Skeletal Muscle Regeneration Is Stimulated by Restorative Macrophages. Stem Cell Rep. 9, 2018-2033, 2017.

19. Desgeorges, T., Liot, S., Lyon, S., Bouviere, J., Kemmel, A., Trignol, A., et al. Open-CSAM, a new tool for semi-automated analysis of myofiber cross-sectional area in regenerating adult skeletal muscle. Skelet Muscle. 9, 2, 2019.

20. Chazaud, B. Macrophages: supportive cells for tissue repair and regeneration. Immunobiology. 219, 172-178, 2014.

21. Meddahi, A., Bree, F., Papy-Garcia, D., Gautron, J., Barritault, D., and Caruelle, J.P. Pharmacological studies of RGTA(11), a heparan sulfate mimetic polymer, efficient on muscle regeneration. J Biomed Mater Res. 62, 525-31, 2002.

22. Natarajan, A., Lemos, D.R., and Rossi, F.M. Fibro/adipogenic progenitors: A double-edged sword in skeletal muscle regeneration. Cell Cycle. 9, 2045-2046, 2010.

23. Barbosa, I., Morin, C., Garcia, S., Duchesnay, A., Oudghir, M., Jenniskens, G., et al. A synthetic glycosaminoglycan mimetic (RGTA) modifies natural glycosaminoglycan species during myogenesis. J Cell Sci. 118, 253-64, 2005.

24. Papy-Garcia, D., Barbosa, I., Duchesnay, A., Saadi, S., Caruelle, J.P., Barritault, D., et al. Glycosaminoglycan mimetics (RGTA) modulate adult skeletal muscle satellite cell proliferation in vitro. J Biomed Mater Res. 62, 46-55, 2002.

25. Zimowska, M., Constantin, B., Papy-Garcia, D., Raymond, G., Cognard, C., Caruelle, J.P., et al. Novel glycosaminoglycan mimetic (RGTA, RGD120) contributes to enhance skeletal muscle satellite cell fusion by increasing intracellular Ca2+ and calpain activity. J Cell Physiol. 205, 237-45, 2005.

Tissue Engineering
Heparan sulfate mimetic accelerate post-injury skeletal muscle regeneration (DOI: 10.1089/ten.TEA.2019.0058)
This paper has been peer-reviewed and accepted for publication, but has yet to undergo copyediting and proof correction. The final published version may differ from this proof.

26. Rouet, V., Hamma-Kourbali, Y., Petit, E., Panagopoulou, P., Katsoris, P., Barritault, D., et al. A synthetic glycosaminoglycan mimetic binds vascular endothelial growth factor and modulates angiogenesis. J Biol Chem. 280, 32792-800, 2005.

27. Chevalier, F., Lavergne, M., Negroni, E., Ferratge, S., Carpentier, G., Gilbert-Sirieix, M., et al. Glycosaminoglycan mimetic improves enrichment and cell functions of human endothelial progenitor cell colonies. Stem Cell Res. 12, 703-15, 2014.

Tissue Engineering
Heparan sulfate mimetic accelerate post-injury skeletal muscle regeneration (DOI: 10.1089/ten.TEA.2019.0058)
This paper has been peer-reviewed and accepted for publication, but has yet to undergo copyediting and proof correction. The final published version may differ from this proof.

Figure legends

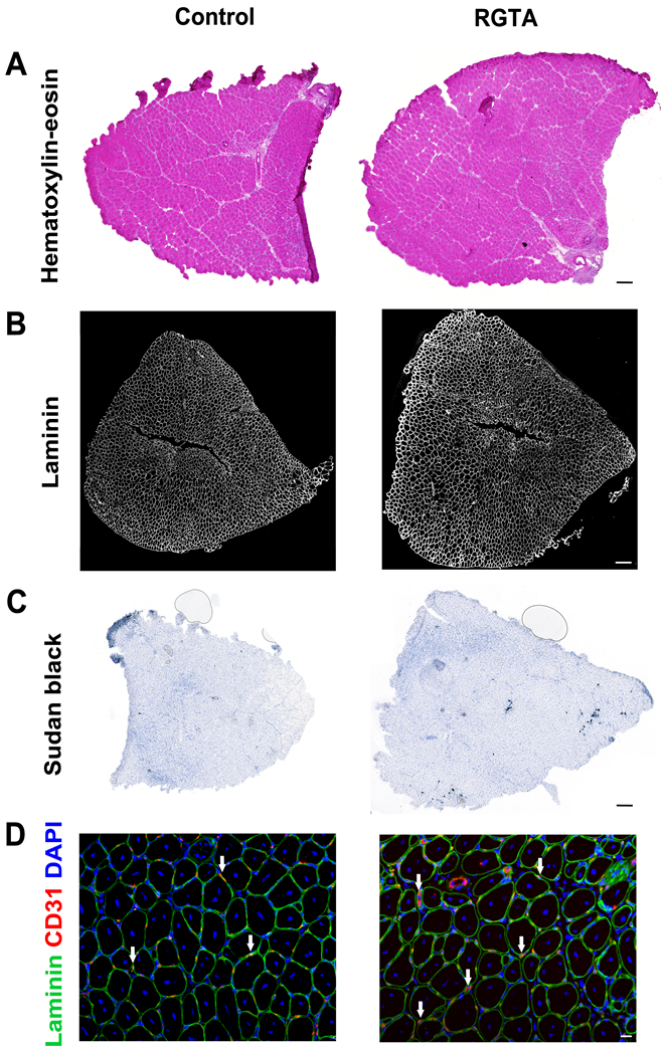

Figure 1 – Analysis of the effects of RGTA® on skeletal muscle regeneration 8 days post injury. RGTA® (1 µg/muscle) was *i.m.* injected 3 days after cardiotoxin injury and muscles were recovered 5 days later. **(A)** Hematoxylin-eosin staining indicating that the whole muscle underwent regeneration. **(B)** Muscle sections were immunolabeled for the detection of laminin (component of the basal lamina) to identify individual myofibers in the regenerating muscle. **(C)** Black Sudan staining was performed to detect adiposis. **(D)** Muscle sections were immunolabeled for the detection of CD31 (vessels, red), laminin (basal lamina, green), and Hoechst (nuclei, blue). White arrows show the capillaries (red). Bar=250µm in A-C. Bar=25µm in D.

Tissue Engineering
Heparan sulfate mimetic accelerate post-injury skeletal muscle regeneration (DOI: 10.1089/ten.TEA.2019.0058)
This paper has been peer-reviewed and accepted for publication, but has yet to undergo copyediting and proof correction. The final published version may differ from this proof.

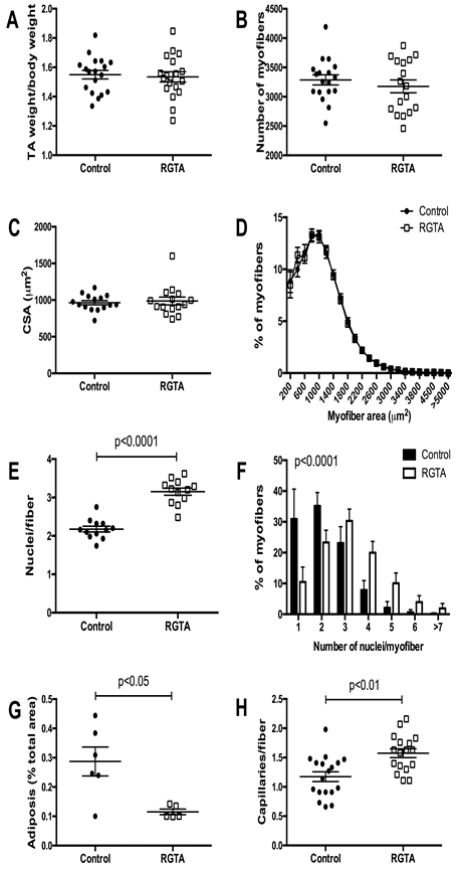

Figure 2 – Effect of RGTA® on skeletal muscle regeneration 8 days post-injury. RGTA® (1 µg/muscle) was *i.m.* injected 3 days after cardiotoxin injury and muscles were recovered 5 days later. **(A)** Muscle weight (mg) of the T*ibialis Anterior* muscle was normalized to the body weight (g). **(B-D)** Muscle sections were immunolabeled for the detection of laminin (as in Figure 1B) and the total number of myofibers (B), the mean Cross Section Area (CSA) (C) and the CSA distribution (D) were calculated using Open-CSAM macro in ImageJ software. **(E-F)** The number of nuclei/myofiber was calculated and given as the mean of the number of nuclei/fiber (E) and as the distribution of myofibers according to the number of nuclei they contain (F). **(G)** Stained area after Black Sudan staining (as in Figure 1C) was reported in % of the total muscle area. **(H)** Muscle sections were immunolabeled for the detection of laminin and of CD31 (as in Figure 1D). The number of $CD31^{pos}$ structures per myofiber was calculated. 3 independent series of experiments including each 3 control (saline injected) and 3 RGTA®-treated mice were performed. Data are given as means ± SEM. T-test was performed except in D and F were 2-way ANOVA was used.

Tissue Engineering
Heparan sulfate mimetic accelerate post-injury skeletal muscle regeneration (DOI: 10.1089/ten.TEA.2019.0058)

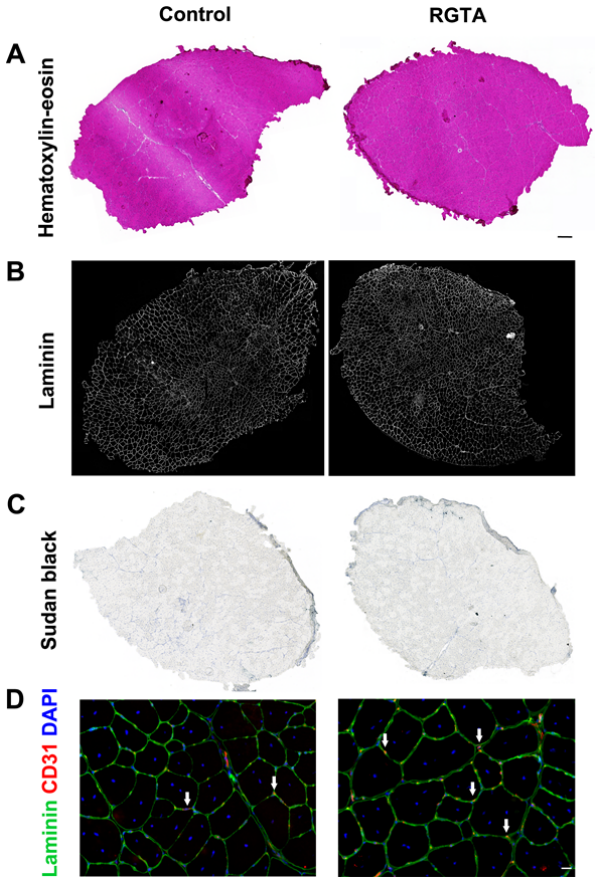

Figure 3 – Analysis of the effects of RGTA® on skeletal muscle regeneration 28 days post injury. RGTA® (1 µg/muscle) was *i.m.* injected 3 days after cardiotoxin injury and muscles were recovered 25 days later. **(A)** Hematoxylin-eosin staining. **(B)** Muscle sections were immunolabeled for the detection of laminin (basal lamina) to identify individual myofibers. **(C)** Black Sudan staining was performed to detect adiposis. **(D)** Muscle sections were immunolabeled for the detection of CD31 (vessels, red), laminin (basal lamina, green), and Hoechst (nuclei, blue). White arrows show the capillaries (red). Bar=250µm in A-C. Bar=25µm in D.

Tissue Engineering
Heparan sulfate mimetic accelerate post-injury skeletal muscle regeneration (DOI: 10.1089/ten.TEA.2019.0058)

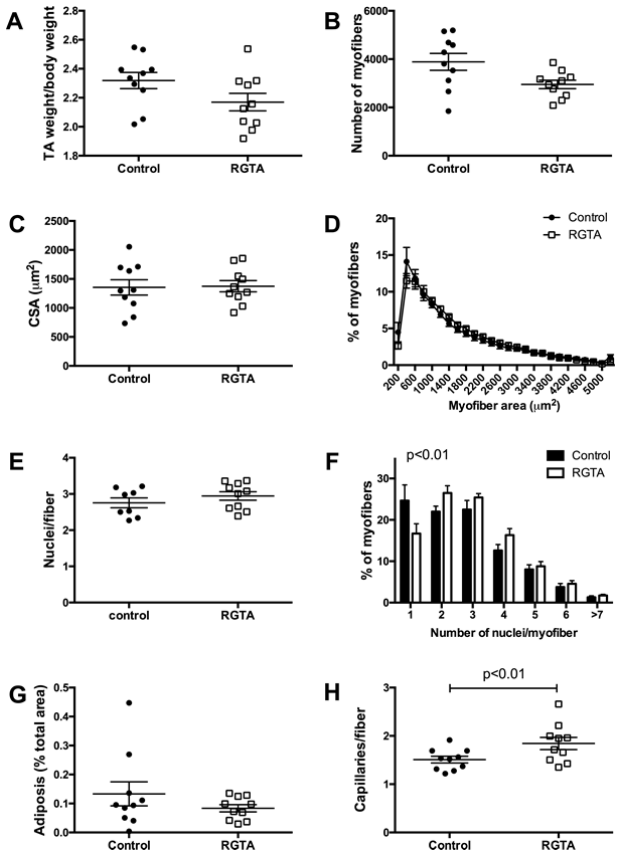

Figure 4 – Effect of RGTA® on skeletal muscle regeneration 28 days post injury. RGTA® (1 µg/muscle) was *i.m.* injected 3 days after cardiotoxin injury and muscles were recovered 25 days later. **(A)** Muscle weight (mg) of the T*ibialis Anterior* muscle was normalized to the body weight (g). **(B-D)** Muscle sections were immunolabeled for the detection of laminin and the total number of myofibers (B), the mean Cross Section Area (CSA) (C) and the CSA distribution (D) were calculated using Open-CSAM macro in ImageJ software. **(E-F)** The number of nuclei/myofiber was calculated and given as the mean of number of nuclei/fiber (E) and as the distribution of myofibers according to the number of nuclei they contain (F). **(G)** Stained area after Black Sudan staining was reported in % of the total muscle area. **(H)** Muscle sections were immunolabeled for the detection of laminin and of CD31. The number of $CD31^{pos}$ structures per myofiber was calculated. Two independent series of experiments including each 3 and 5 control (saline injected) and 3 and 5 RGTA®-treated mice were performed. Data are given as means ± SEM. T-test was performed except in D and F were 2-way ANOVA was used.

Tissue Engineering
Heparan sulfate mimetic accelerate post-injury skeletal muscle regeneration (DOI: 10.1089/ten.TEA.2019.0058)
This paper has been peer-reviewed and accepted for publication, but has yet to undergo copyediting and proof correction. The final published version may differ from this proof.

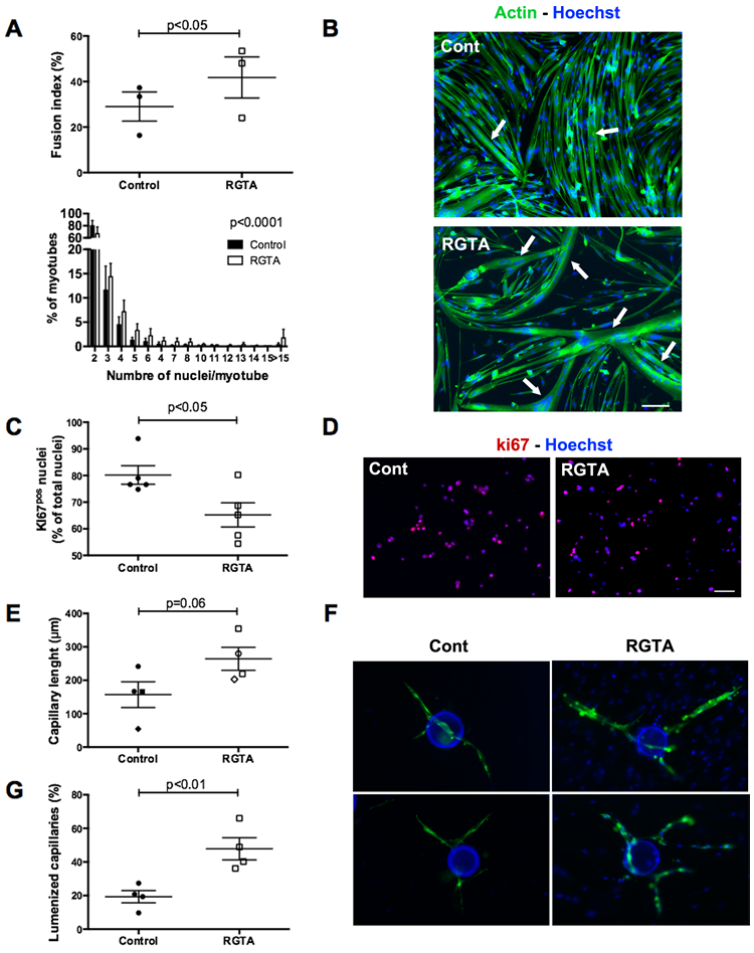

Figure 5 – Effect of RGTA® on *in vitro* myogenesis and angiogenesis. **(A-B)** RGTA® (10 µg/ml) was added to MuSC cultures at the time of differentiation and MuSC fusion was assessed 3 days later after actin staining with phalloidin (green) and was expressed as the fusion index and as the distribution of myotubes according to the number of nuclei they contain. White arrows in B show multinucleated myotubes. **(C-D)** RGTA® (10 µg/ml) was added to MuSC cultures during proliferation and ki67 immunolabeling (red) was performed one day later. The number of cycling (ki67^{pos}) cells was expressed in % of total cells. **(E-G)** RGTA® (10 µg/ml) was added to GFP-expressing endothelial cell 3D cultures and angiogenesis was assessed 6 days later. Endothelial cell (green) sprouting (capillary length, E) and differentiation (lumenized capillaries, G) were evaluated. Blue=Hoechst. Bar=100 µm. Independent experiments performed on different primary MuSC cultures were performed (n=5 in A, n=3 in C, n=4 in E). Data are given as means ± SEM. T-test was performed except in lower panel A were 2-way ANOVA was used.